JPhys Materials

PAPER • OPEN ACCESS

Strong correlation between mobility and magnetoresistance in Weyl and Dirac semimetals

To cite this article: Sukriti Singh *et al* 2020 *J. Phys. Mater.* **3** 024003

JPhys Materials

OPEN ACCESS

RECEIVED
8 October 2019

REVISED
11 December 2019

ACCEPTED FOR PUBLICATION
15 January 2020

PUBLISHED
25 February 2020

PAPER

Strong correlation between mobility and magnetoresistance in Weyl and Dirac semimetals

Sukriti Singh, Vicky Süβ, Marcus Schmidt, Claudia Felser and Chandra Shekhar

Max Planck Institute for Chemical Physics of Solids, D-01187 Dresden, Germany

E-mail: shekhar@cpfs.mpg.de

Keywords: Weyl semimetal, high mobility, magnetoresistance

Abstract

The discovery of Weyl and Dirac fermions in solid systems is a recent major breakthrough in the field of condensed matter physics. These materials exhibit extraordinary properties in terms of carrier mobility and magnetoresistance (MR). These two quantities are highly dependent in the Weyl semimetal transition monopnictide family, i.e. NbP, TaP, NbAs, and TaAs. Furthermore, the gathered mobility and MR (or slope of MR) at 2 K in 9 T of other well-known Weyl and Dirac semimetals follow a relation similar to the *right turn* symbol, i.e. the MR increases rapidly with mobility; thereafter it begins to saturate after reaching a value of 10^3. This suggests a nonlinear dependency. Nevertheless, for materials possessing high carrier mobility, it is valid to expect high MR.

1. Introduction

Mobility refers to the velocity acquired by the charge carrier in a unit of electric field, whereas magnetoresistance (MR) indicates the extent of the resistance change on applying a magnetic field. These two effects are highly pronounced in semimetals, because the valence band maximum and conduction band minimum lie close to the Fermi level, and the charge carriers do not require significant energy to move. This means that the changes are sensitive even if there are small perturbations and that these changes are easily visible in the physical properties. Recently, the topology of materials has attracted tremendous research attention, and it is currently a leading research area in the fields of condensed matter physics and material science [1–10]. Similar to topological insulators, semimetals are also topologically protected, nontrivial metallic phases of matter; this nontrivial topological nature guarantees the existence of exotic Fermi surface as a Fermi arc [2–5]. Owing to the semimetallic character of materials, the conduction and valence bands generally cross each other near the Fermi energy. Depending on their degeneracy, topological semimetals are further distinguished and classified into Weyl semimetals (WSM) and Dirac semimetals. The discovery of Weyl fermions in transition metal monopnictides [1–6] has facilitated the discovery of additional Dirac and Weyl semimetals in the various families of compounds [11–27].

Unlike their family and class, topological semimetals exhibit significantly high mobility and MR, accompanied by a low effective mass of the charge carrier. This low effective mass results in a high mobility; thus, the material reaches the quantum limit in a moderate magnetic field. In this condition, the resistivity of materials varies linearly with the magnetic field, resulting in a linear MR, which is known as quantum MR [28]. Among topological materials, the number of compounds that exhibit linear MR is comparatively low [14–16, 19]. Generally, MR deviates from linearity in a majority of the compounds and exhibits parabolic behaviour due to the charge carrier compensation [11–13, 17, 18, 20–27]. An excellent example of parabolic MR is exhibited by type-II Weyl semimetals, in which unavoidably Fermi level possesses through the tilted Weyl cone and simultaneously creates electron and hole bands [12, 13, 23]. Irrespective of the MR behaviour, the fluctuations in mobility arising due to disorder or inhomogeneity is another phenomenon that occurs in a wide range of materials [29]. Here, we investigate the relation between MR and mobility by considering the example of Weyl semimetal transition metal monopnictides. Based on the data of the best-known Weyl and Dirac semimetals

(or slope of MR) at ~2 K in 9 T presented in literature, the mobility and MR are correlated, and they follow the 'right turn' symbol, i.e. MR increases rapidly and thereafter begins to saturate after reaching the value of 10^3.

2. Experimental details

Single crystals of NbP, TaP, NbAs, and TaAs were grown via chemical vapour transport [30, 31]. As a first step for polycrystalline material, stoichiometric quantities of Nb, Ta (Alfa Aesar, 99.99%), P (Alfa Aesar, 99.999%), and As (Chempur, 99.9999%) were accurately weighed in a quartz ampoule. Thereafter, they were flushed with Ar, sealed under vacuum, and the sealed quart tube was heated in two consecutive temperatures, i.e. 600 °C and 800 °C, for 24 h. In the next step to grow the crystals, we used the microcrystalline powders from step one and added iodine (7–8 mg ml^{-1}) before sealing the powders in a quartz tube. The crystal was grown in a two-zone furnace at a temperature range of 900 °C–1050 °C, for 2–4 weeks. Here, I_2 acts as a transport agent. To obtain high quality crystals, the temperature gradient is one of the most important parameters, and it varies based on the material. We optimized the temperature gradient for each material mentioned in the present investigation. It is 900 °C (source)–1000 °C (sink) for NbP and TaP and 900 °C (source)–1050 °C (sink) for NbAs and TaAs. Additional details regarding crystal growth and their characterization can be found in our previous studies [6, 32–34]. The experimental lattice parameters of the four compounds are $a = 3.3314(8)$ Å and $c = 11.3649(3)$ Å for NbP, $a = 3.3166(9)$ Å and $c = 11.3304(6)$ Å for TaP, $a = 3.4492(6)$ Å and $c = 11.6647(3)$ Å for NbAs, and $a = 3.4310(4)$ Å and $c = 11.6252(6)$ Å for TaAs. These values are similar to those in previous reports [35, 36]. The resistivity measurements were performed in Quantum Design-physical property measurement system in the AC-Transport options. Our well characterized crystals were cut into bar-shapes by using the wire saw and keeping the longest length along the crystallographic *a*-axis, in which direction the current was applied in resistivity measurements. The physical dimensions are 3.1 mm × 1.6 mm × 0.56 mm for NbP, 1.1 mm × 0.42 mm × 0.16 mm for TaP, 0.93 mm × 0.83 mm × 0.17 mm for NbAs, and 1.5 mm × 0.42 mm ×0.28 mm for TaAs. The measurements for resistivity and Hall resistivity were performed in four and five-probe geometries, respectively, for a constant current source of 3–4 mA.

3. Results and discussion

The resistivity, ρ_{xx} of all crystals at the zero field decreases with decreasing temperature, which is an expected characteristic of metallic compounds. Their low residual resistivity and high residual resistivity ratio values reflect the high quality of the crystals [6]. Apart from the well-established Weyl property, these compounds are also well known for exhibiting ultrahigh mobility and MR. We now focus on the measurements for MR. Generally, MR is calculated as the ratio of the change in resistivity due to the applied magnetic field and the initial resistivity, using the relation $MR = \rho_{xx}(B) - \rho_{xx}(0)/\rho_{xx}(0)$, where B is applied magnetic field perpendicular to current. On the contrary, mobility is estimated based on the slope of Hall resistivity at the high magnetic field region, where it is almost linear with the field at different temperatures. The measured MR of NbP, TaP, NbAs, and TaAs at the selected temperatures are shown in figure 1. The most noteworthy features are

(i) Positive and unsaturating MR that exhibits systematic variations with the temperature and field.

(ii) The MR is almost constant up to 50 K, whereas it decreases sharply above 50 K.

(iii) More importantly, all the compounds exhibit Shubnikov de-Haas (SdH) oscillations below 20 K, thereby reflecting the high quality of the crystals.

A detailed analysis of the SdH oscillations and their fermiology can be found in previous literature [6, 32]. Among the four compounds, NbP exhibits the highest MR of 8.5×10^5 % at 1.85 K, in a field of 9 T. Additionally, it does not exhibit any sign of saturation under ultrahigh fields of 62 T, at 1.5 K [6]. This value is five times higher than the value that was reported for WTe_2, which is another WSM, in the same field [12]. The MR of NbP is as high as 250% even at 300 K and 9 T (inset of figure 1(a)). Moreover, the other members of this series also exhibit similar MR orders as that of NbP at all temperature and field ranges [37, 38]. In the presence of magnetic fields, a nonzero transverse current experiences a Lorentz force in the inverse-longitudinal direction. Such a back flow of carriers eventually increases the apparent longitudinal resistance, resulting in an extremely high MR. From the above mentioned measurements, we can conclude that these materials have a unique property of high and never saturating MR.

We now focus on mobility, which can be derived from the measurements of Hall resistivity, ρ_{xy}, which is further defined as $\rho_{yx} = V_y.t/I_x$, where V_y is the voltage developed normal to the applied magnetic field and current I_x and t is the thickness of the crystal. The carrier mobility and concentration usually derived

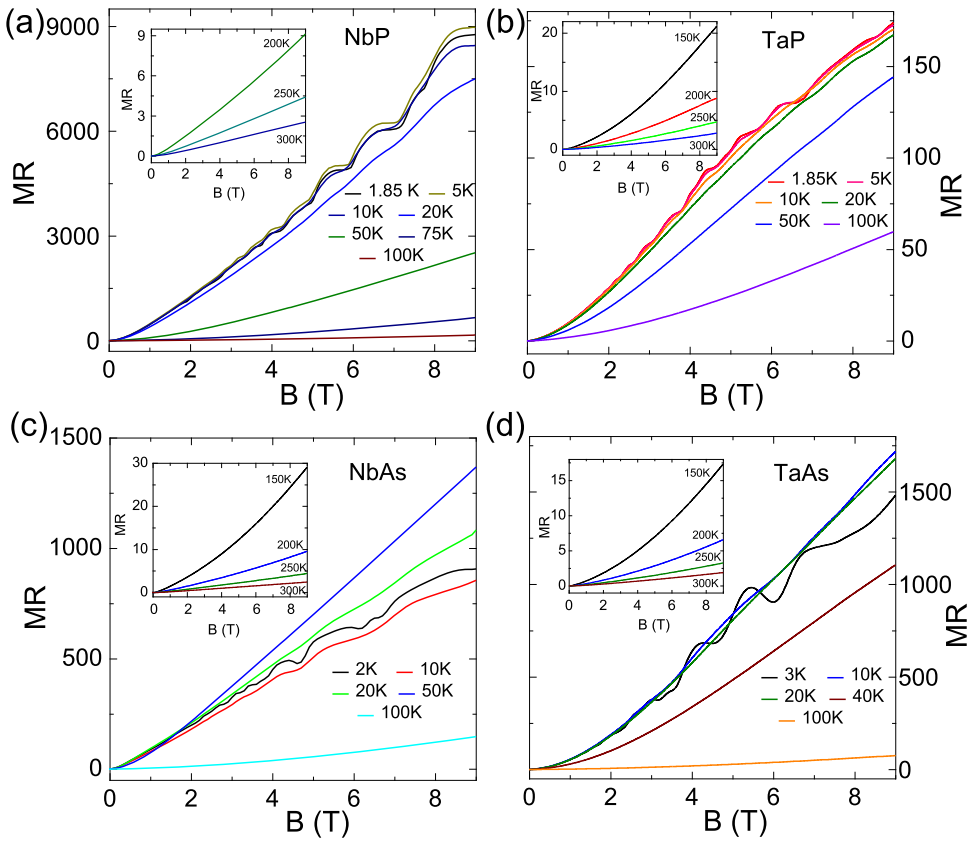

Figure 1. Estimated transverse magnetoresistance at different temperatures from the field dependent resistivity using $MR = \rho_{xx}(B) - \rho_{xx}(0)/\rho_{xx}(0)$ for (a) NbP, (b) TaP, (c) NbAs, (d) TaAs. Inset show their respective magnetoresistance at high temperature $\geqslant$150 K.

from ρ_{yx} are two important parameters of a material. We have performed Hall measurements in the positive and negative field directions to improve the accuracy of data. For the sake of simplicity, we used the single-carrier Drude model, $\mu_{avg}(T) = R_H(T)/\rho_{xx}(T)$, where $\mu_{avg}(T)$ is the average mobility, and $R_H(T)$ is the Hall coefficient calculated from the linear slope of $\rho_{yx}(T)$ at the high field. However, the sign of the Hall coefficient changes from negative to positive between 125 and 170 K, depending on the material, e.g. this temperature is approximately 125 K for Nb-compounds [6] and 170 K for Ta-compounds [32]. The charge carrier density lies between 10^{18} and 10^{20} cm^{-3} in the temperature range of 2–300 K. The observed small carrier density at low temperatures and its significant change on increasing the temperature are typical characteristics of semimetals. A large MR is usually associated with high mobility, and it plays a major role in the charge transport in a material. Consequently, it determines the efficiency of devices. We calculated the average mobility and plotted it against temperature, as shown in figure 2. It is evident that NbP exhibits the highest mobility of 5×10^6 cm^2 V^{-1} s^{-1} and the lowest residual resistivity of 0.63 $\mu\Omega$ cm at 2 K. These values are similar to those of Cd_3As_2 [15]. The mobilities of the other members are 3×10^5 cm^2 V^{-1} s^{-1} for TaP, 5×10^5 cm^2 V^{-1} s^{-1} for NbAs, and 4×10^5 cm^2 V^{-1} s^{-1} for TaAs, at 2 K. Their residual resistivities are 3.2 $\mu\Omega$ cm for TaP, 6.2 $\mu\Omega$ cm for NbAs, and 4.2 $\mu\Omega$ cm for TaAs. It is noteworthy that the estimated mobility from a single-carrier model only differs slightly from the mobility obtained from the two-carrier model; consequently, its overall temperature dependent behaviour remains almost the same. From the above mentioned values of mobility and residual resistivity, it is clear that an anomalously low residual resistivity can be achieved in a clean system where the mobility attains ultrahigh values. When the magnetic field is applied, the low temperature resistivity increases steeply, resulting in a significantly large MR [6, 12, 32]. To examine the role of the mobility on MR, we calculated the slope of the MR at approximately 9 T, and the mobility at different temperatures for NbP, TaP, NbAs, and TaAs. The slope $\partial MR/\partial B$ is plotted on the right axis, and the carrier mobility is plotted on the left axis as a function of temperature, as shown in figure 2. $\partial MR/\partial B$ and μ_{avg} exhibit identical variation with temperature, indicating that MR is governed by the mobility, at least in these four compounds. A slight deviation of the mobility graph in the range 100–200 K belongs to the region where the majority of charge carriers switch from electrons to holes. We conclude that the average mobility and MR are well correlated for all the four compounds.

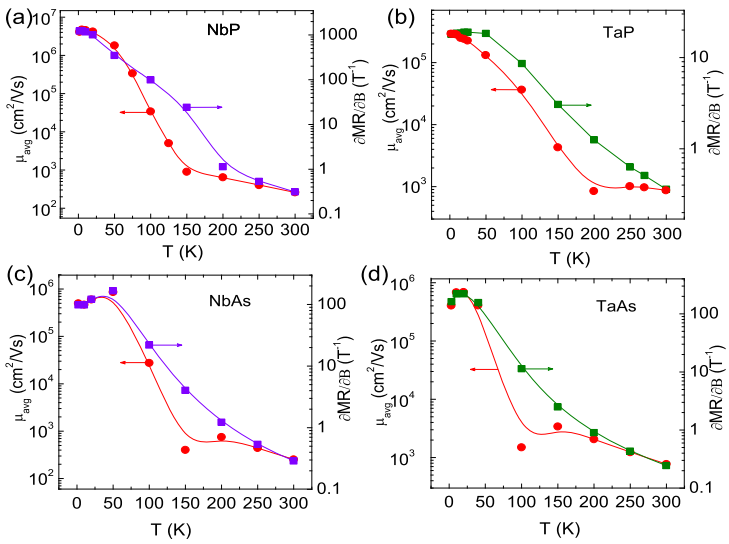

Figure 2. Temperature dependent average mobility, μ_{avg} (left axis) from single carrier model and slope of magnetoresistance (right axis) around 9 T field for (a) NbP, (b) TaP, (c), NbAs and (d) TaAs. From the two-carrier model, the obtained mobility is similar as single-carrier model, and therefore its temperature dependent does not alter much.

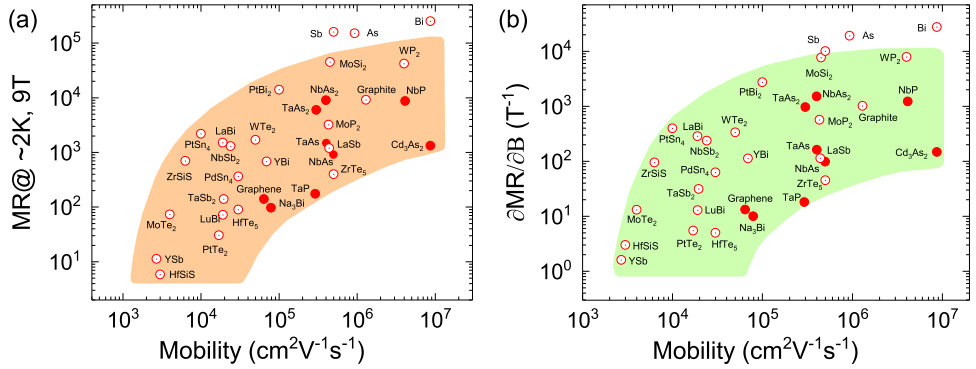

Figure 3. Magnetoresistance (MR) and mobility of various well-known Weyl and Dirac semimetals at ~2 K. (a) MR in 9 T versus mobility. (b) Slope of MR around 9 T versus mobility. The compounds with filled circle show linear MR. The data were taken from the [11–27, 39–43].

We generalize our findings for a broader range of Weyl and Dirac semimetals. It is essential to examine the variability in MR with respect to the mobility in these compounds. We gathered these two quantities for various compounds at ~2 K and 9 T from literature [11–27, 39–42]. As MR varies with the field, it is more valid to consider the slope of the MR with the field than considering the value of MR in a fix field. However, we plotted MR and its slope at approximately 9 T against the mobility at 2 K, as shown in figures 3(a) and (b), respectively. The behaviour of both the graphs is highly similar, and both show an intriguing relation between MR and mobility. The MR initially increases sharply with mobility, and thereafter it begins to saturate after reaching the value of 10^3, forming a shape similar to the *right turn* symbol. Nevertheless, this relation broadly confirms that high mobility compounds possess high MR. It seems that this right turn behavior is limited to charge carrier density. A group of compounds with similar order of mobility (for example, WP_2, $MoSi_2$ and $NbAs_2$) but the high carrier density possess high MR while the low carrier density compounds (for example, Cd_3As_2, $ZrTe_5$ and NbAs) show low MR. This approximation can be understood in term of charge saturation in quantum limit in which the semimetals with lower carrier density get easily saturated at rather lower field, exhibiting lower MR compared to the semimetals with higher carrier density. Noticeably, in the presence of magnetic fields, a high mobile carrier experience a stronger Lorentz force, and exhibits high MR. However, it appears that apart from this, some other factors also contribute to the Lorentz force, otherwise MR would be linearly related to the mobility.

4. Conclusion

To summarize, we demonstrate the dependence of MR and mobility on temperature by considering the examples of transition metal−monopnictides Weyl semimetals. We also show that a similar dependency may exist in other compounds. The plots between the MR or the slope of MR versus the mobility of the most popular Weyl and Dirac semimetals exhibit a shape similar to the *right turn* symbol, i.e. the MR increases sharply and thereafter undergoes saturation after reaching 10^3. Our analyses reveal that the MR highly depends on mobility, and a high MR can be expected in high carrier mobility compounds.

Acknowledgments

This work was supported by the Deutsche Forschungsgemein- schaft DFG (SFB 1143) and by the ERC Advanced grant 742068 'TOPMAT'.

ORCID iDs

Chandra Shekhar https://orcid.org/0000-0002-3330-0400

References

[1] Weng H, Fang C, Fang Z, Bernevig B A and Dai X 2015 *Phys. Rev.* X **5** 011029
[2] Xu S-Y *et al* 2015 *Nat. Phys.* **11** 748–54
[3] Yang L X *et al* 2015 *Nat. Phys.* **11** 728–32
[4] Lv B Q *et al* 2015 *Phys. Rev.* X **5** 031013
[5] Liu Z K *et al* 2016 *Nat. Mater.* **15** 27–31
[6] Shekhar C *et al* 2015 *Nat. Phys.* **11** 645–9
[7] Bradlyn B, Cano J, Wang Z, Vergniory M G, Felser C, Cava R J and Bernevig B A 2016 *Science* **353** aaf5037
[8] Armitage N P, Mele E J and Vishwanath A 2018 *Rev. Modern Phys.* **90** 015001
[9] Hu J, Xu S-Y, Ni N and Mao Z 2019 *Ann. Rev. Mater. Res.* **49** 207–52
[10] Gao H, Venderbos J W F, Kim Y and Rappe A M 2019 *Ann. Rev. Mater. Res.* **49** 153–83
[11] Mun E, Ko H, Miller G J, Samolyuk G D, Bud'ko S L and Canfield P C 2012 *Phys. Rev.* B **85** 035135
[12] Ali M N *et al* 2014 *Nature* **514** 205–8
[13] Keum D H *et al* 2015 *Nat. Phys.* **11** 482
[14] Tafti F F, Gibson Q D, Kushwaha S K, Haldolaarachchige N and Cava R J 2015 *Nat. Phys.* **12** 272
[15] Liang T, Gibson Q, Ali M N, Liu M, Cava R J and Ong N P 2015 *Nat. Mater.* **14** 280–4
[16] Yuan Z, Lu H, Liu Y, Wang J and Jia S 2016 *Phys. Rev.* B **93** 184405
[17] Kumar N, Shekhar C, Wu S-C, Leermakers I, Young O, Zeitler U, Yan B and Felser C 2016 *Phys. Rev.* B **93** 241106
[18] Ali M N, Schoop L M, Garg C, Lippmann J M, Lara E, Lotsch B and Parkin S 2016 *Sci. Adv.* **2** e1601742
[19] Xiong J, Kushwaha S, Krizan J, Liang T, Cava R J and Ong N P 2016 *Europhys. Lett.* **114** 17002
[20] Pavlosiuk O, Swatek P and Wiśniewski P 2016 *Sci. Rep.* **6** 18691
[21] Jo N H *et al* 2017 *Phys. Rev.* B **96** 165145
[22] Gao W *et al* 2017 *Phys. Rev. Lett.* **118** 256601
[23] Kumar N *et al* 2017 *Nat. Commun.* **8** 1642
[24] Kumar N, Manna K, Qi Y, Wu S-C, Wang L, Yan B, Felser C and Shekhar C 2017 *Phys. Rev.* B **95** 121109
[25] Leahy I A, Lin Y-P, Siegfried P E, Treglia A C, Song J C W, Nandkishore R M and Lee M 2018 *Proc.Natl Acad. Sci.* **115** 10570–5
[26] Matin M, Mondal R, Barman N, Thamizhavel A and Dhar S K 2018 *Phys. Rev.* B **97** 205130
[27] Pavlosiuk O and Kaczorowski D 2018 *Sci. Rep.* **8** 11297
[28] Abrikosov A A 1998 *Phys. Rev.* B **58** 2788–94
[29] Parish M M and Littlewood P B 2003 *Nature* **426** 162–5
[30] Schäfer H and Fuhr W 1965 *J. Less Common Met.* **8** 375–87
[31] Martin J and Gruehn R 1988 *Z. Kristallogr.* **182** 180–2
[32] Arnold F *et al* 2016 *Nat Commun* **7** 11615
[33] dos Reis R D, Wu S C, Sun Y, Ajeesh M O, Shekhar C, Schmidt M, Felser C, Yan B and Nicklas M 2016 *Phys. Rev.* B **93** 205102
[34] Klotz J *et al* 2016 *Phys. Rev.* B **93** 121105
[35] Boller H and Parthe E 1963 *Acta Crystallogr.* **16** 1095–101
[36] Saini G S, Calvert L D and Taylor J B 1964 *Can. J. Chem* **42** 630–4
[37] Huang X *et al* 2015 *Phys. Rev.* X **5** 031023
[38] Ghimire N J, Luo Y, Neupane M, Williams D J, Bauer E D and Ronning F 2015 *J. Phys.: Condens. Matter.* **27** 152201
[39] Fauqué B, Yang X, Tabis W, Shen M, Zhu Z, Proust C, Fuseya Y and Behnia K 2018 *Phys. Rev. Mater.* **2** 114201
[40] Zhao L, Xu Q, Wang X, He J, Li J, Yang H, Long Y, Chen D, Liang H and Li C 2017 *Phys. Rev.* B **95** 115119
[41] Soule D 1958 *Phys. Rev.* **112** 698
[42] Li P, Zhang Q, He X, Ren W, Cheng H-M and Zhang X-X 2016 *Phys. Rev.* B **94** 045402
[43] Pavlosiuk O, Swatek P, Kaczorowski D and Wiśniewski P 2018 *Phys. Rev.* B **97** 235132